Structural and Magnetic Characterization of Tetranuclear [Ni(II)$_2$Ln(III)$_2$] Complexes Bearing Tetra-branched Schiff base ligands

Lingyi Shen,[a,b‡] Peng Hu,[c‡] Xian-Jiong Yang,[a,b] Hong Xu,[b] Ya-Li Huang,[b] Carl Redshaw[d]* and Qi-Long Zhang[a,b]*

[a] *School of Public Health, the key Laboratory of Environmental Pollution Monitoring and Disease Control, Ministry of Education, Guizhou Medical University, Guiyang 550014, China.*

[b] *Research Center for Molecular Medical Engineering, School of Basic Medical Science, Guizhou Medical University, Guiyang 550004, China.*

[c] *Hubei Key Laboratory of Radiation Chemistry and Functional Materials, Non-power Nuclear Technology Collaborative Innovation Center, Hubei University of Science and Technology, Xianning 437100, China.*

[d] *Department of Chemistry, University of Hull, Cottingham Road, Hull, Yorkshire HU6 7RX, UK. c.redshaw@hull.ac.uk*

‡ *These authors contributed equally to this work.*

Abstract: A series of tetranuclear [Ni(II)$_2$Ln(III)$_2$] complexes of general formula [Ni$_2$Ln$_2$(**L**)(H$_2$O)$_9$(OH)$_4$Cl]·3H$_2$O·Cl (**1**, **2**, **5**) (Ln = Dy (**1**), Tb (**2**), Ho (**5**)) and [Ni$_2$Ln$_2$(**L**)(H$_2$O)$_{12}$Cl] ·3H$_2$O·5Cl (**3**, **4**, **6**, **7**) (Ln = Gd (**3**), Sm (**4**), Nd (**6**), Pr (**7**)); H$_4$**L** = *N*,*N*',*N*'',*N*'''-tetra(3-methoxysalicylidene)-pentaerythritol) have been synthesized. The molecular structures and magnetic properties of **1**−**7** are reported. Structural analysis indicated that this family of clusters consists of a tetranuclear [Ni(II)$_2$Ln(III)$_2$] core, supported by a tetrapodal Schiff base ligand. Both Ni(II) ions adopt a distorted octahedral coordination environment, whilst the two terminal Ln(III) ions exhibit distorted tricapped trigonal prismatic geometries and are coordinated by eight or nine oxygen donor atoms. Magnetic measurements revealed that the Dy derivative of

complex **1** displays typical d single-molecule magnet behaviour with the presence of slow magnetic relaxation. By contrast, complexes **2**−**7**, no obvious SMM behaviour was exhibited, however for the Gd derivative **3**, a significant magnetocaloric effect was observed.

Keywords: Structural analysis; Schiff base; Magnetic measurements; Single-molecule magnet; magnetocaloric effect

1. Introduction

Polynuclear heterometallic coordination clusters consisting of lanthanide metal ions have fuelled research activity in the field of molecular magnetism due to their ability to behave as single-molecule magnets (SMMs) [1] and low-temperature molecular magnetic coolers (MMCs) [2]. Anisotropic Ln(III) ions, such as Dy(III) ions, are ideal spin centres to assemble polynuclear SMMs that have potential application in high-density information storage and molecular spintronics [3], while Gd ion comprised clusters are likely to perform magnetocaloric effects thereby providing promising applications in ultra-low temperature cooling owing to the magnetic isotropy and high spin state [4].

In terms of molecule-based magnets, the SMM behaviour can be usually promoted by an axially symmetric crystal field around the 4f ions and strong exchange coupling between paramagnetic centres. Given the efficient shielding of the 4f orbitals of the Ln(III) ion by the fully occupied 5s and 5p orbitals, 3d−4f heterometallic clusters have been considered as effective SMM candidates because of the combination of the strong magnetic interactions introduced by 3d transition metal ions and large anisotropies endowed by 4f metal ions [5]. Moreover, 3d ions like Ni(II) can also make some contribution to the magnetic anisotropy in the 3d – 4f system, due to its second-order orbital angular momentum. Accordingly, an increasing number of Ni−Ln polynuclear complexes

have been reported in recent years [6], but only a few of them show SMM behaviour [7], while the MMC properties of their Ni–Gd analogues have been barely studied.

The selection of the chelating ligands plays a crucial role in constructing 3d–4f clusters with desirable properties. It is generally agreed that Schiff base derivatives condensed by *o*-vanillin and amine possessing multiple coordination sites and flexible skeletons are excellent candidates to match the structural requirements. The *N*–*O* chelating sites show an inclination for 3d metal ions, while the 'coordination pockets' featuring the phenolic hydroxyl and methoxy groups favour hard oxyphilic 4f metal ions [8]. Numerous Schiff base derivatives, prepared by reacting *o*-vanillin with monamine or diamine have been utilized to construct 3d–4f clusters [9], but triamine or tetramine derived complexes are rarely used to synthesize these types of systems.

With the above considerations in mind, we have selected the tetra-branched Schiff base ligand H_4**L** (Scheme 1) as our entry point to explore new 3d–4f magnetic clusters. Herein, seven new tetranuclear 3d–4f heterometallic complexes based on this multidentate ligand have been successfully constructed, and have been found to exhibit similar twisted butterfly-like structures. Magnetic studies reveal that the Gd derivative exhibits a significant magnetic entropy change, and the Dy derivative exhibits slow magnetic relaxation, and this is the first SMM system based on such a tetra-branched Schiff base derivative. Herein, the synthesis, structural and magnetic studies of these tetranuclear [Ni(II)$_2$Ln(III)$_2$] clusters are described.

2. Experimental

2.1 General

All of the starting materials and solvents were commercially available and were used without further purification. Ultrapure water was used throughout the experiments. ^{1}H NMR spectra were measured using an Inova-400 Bruker AV 400 spectrometer (Bruker, Karlsruhe, Germany) at room

temperature. DMSO-d_6 was used as a solvent and tetramethylsilane (TMS) as an internal standard. Single crystal X-ray diffraction was conducted on a Bruker Smart Apex II single crystal diffractometer (Bruker, Karlsruhe, Germany).

2.2 X-ray Crystallography

Diffraction data for the complexes **1**−**7** were collected on a Bruker SMART APEX II diffractometer at room temperature (298 K) with graphite-monochromated Mo/Kα radiation (λ = 0.71073 Å). An empirical absorption correction using SADABS was applied for all data [10]. The structures were solved and refined to convergence on F2 for all independent reflections by the full-matrix least squares method using the SHELXL−2014 programs [11] and OLEX2 1.2 [12]. Hydrogen atoms bonded to carbons were included in idealized geometric positions with thermal parameters equivalent to 1.2 times those of the atom to which they were attached. There is a large amount of solvent water molecule disorder in complexes **1**-**7** and some water molecules were removed using the SQUEEZE routine implemented within the software program PLATON [13], and the resulting .fab file was processed with OLEX2 1.2 using the ABIN instruction, which caused the observed level B alerts. Specific details of the SQUEEZE treatment for each complex is given in the ESI. Crystallographic data and refinement details for the complexes **1**-**7** are given in Table S1 and Table S2.

2.3 Synthesis of $[Ni_2Dy_2(\mathbf{L})(H_2O)_9(OH)_4Cl]\cdot 3H_2O\cdot Cl$ (**1**$\cdot 3H_2O\cdot Cl$)

The compound of $H_4\mathbf{L}$ was synthesized according to the previously reported method [14]. To a stirred solution of $H_4\mathbf{L}$ (337.9 mg, 0.5 mmol) in chloroform (150 mL) was added 20 mL $Ni(Ac)_2\cdot 4H_2O$ (248.8 mg, 1.0 mmol) in ethanol solution (20 mL), and the mixture was stirred for 2 h, the resulting mixture was filtered to afford brown powdered $Ni_2\mathbf{L}$, which was washed by ethanol (30 mL). The $Ni_2\mathbf{L}$ (391.2 mg, 0.5 mmol) and $DyCl_3\cdot 6H_2O$ (376.9 mg, 1.0 mmol) were

mixed in ethanol (150 mL) and stirred for 8 h. The filtrate was evaporated over two days to afford X-ray quality dark green crystals in a yield of 43.2%.

2.4 Synthesis of $[Ni_2Tb_2(\mathbf{L})(H_2O)_9(OH)_4Cl]\cdot 3H_2O\cdot Cl$ (**2**$\cdot 3H_2O\cdot Cl$)

This complex was prepared in a manner analogous to that of **1**, except that $TbCl_3\cdot 6H_2O$ (373.4 mg, 1.0 mmol) was used instead of $DyCl_3\cdot 6H_2O$. The filtrate was evaporated over two days providing X-ray quality dark green block crystals of **2**$\cdot 3H_2O\cdot Cl$ in a yield of 32.2%.

2.5 Synthesis of $[Ni_2Gd_2(\mathbf{L})(H_2O)_{12}Cl]\cdot 3H_2O\cdot 5Cl$ (**3**$\cdot 3H_2O\cdot 5Cl$)

This complex was prepared in a manner analogous to that of **1**, except that $GdCl_3\cdot 6H_2O$ (371.8 mg, 1.0 mmol) was used instead of $DyCl_3\cdot 6H_2O$. The filtrate was evaporated for two weeks providing X-ray quality dark green block crystals of **3**$\cdot 3H_2O\cdot 5Cl$ in a yield of 41.2%.

2.6 Synthesis of $[Ni_2Sm_2(\mathbf{L})(H_2O)_{12}Cl]\cdot 3H_2O\cdot 5Cl$ (**4**$\cdot 3H_2O\cdot 5Cl$)

This complex was prepared in a manner analogous to that of **1**, except that $SmCl_3\cdot 6H_2O$ (364.8 mg, 1.0 mmol) was used instead of $DyCl_3\cdot 6H_2O$. The filtrate was evaporated for two weeks providing X-ray quality dark green block crystals of **4**$\cdot 3H_2O\cdot 5Cl$ in a yield of 42.5%.

2.7 Synthesis of $[Ni_2Ho_2(\mathbf{L})(H_2O)_9(OH)_4Cl]\cdot 3H_2O\cdot Cl$ (**5**$\cdot 3H_2O\cdot Cl$)

This complex was prepared in a manner analogous to that of **1**, except that $HoCl_3\cdot 6H_2O$ (308.5 mg, 1.0 mmol) was used instead of $DyCl_3\cdot 6H_2O$. The filtrate was evaporated for two weeks providing X-ray quality dark green block crystals of **5**$\cdot 3H_2O\cdot Cl$ in a yield of 38.9%.

2.8 Synthesis of $[Ni_2Nd_2(\mathbf{L})(H_2O)_{12}Cl]\cdot 3H_2O\cdot 5Cl$ (**6**$\cdot 3H_2O\cdot 5Cl$)

This complex was prepared in a manner analogous to that of **1**, except that $NdCl_3 \cdot 6H_2O$ (358.7 mg, 1.0 mmol) was used instead of $DyCl_3 \cdot 6H_2O$. The filtrate was evaporated for two weeks providing X-ray quality dark green block crystals of **6**$\cdot 3H_2O \cdot 5Cl$ in a yield of 43.6%.

2.9 Synthesis of $[Ni_2Pr_2(\mathbf{L})(H_2O)_{12}Cl] \cdot 3H_2O \cdot 5Cl$ (**7**$\cdot 3H_2O \cdot 5Cl$)

This complex was prepared in a manner analogous to that of **1**, except that $PrCl_3 \cdot 6H_2O$ (355.4 mg, 1.0 mmol) was used instead of $DyCl_3 \cdot 6H_2O$. The filtrate was evaporated for two weeks providing X-ray quality dark green block crystals of **7**$\cdot 3H_2O \cdot 5Cl$ in a yield of 39.5%.

2.10 Magnetic measurements

Magnetic susceptibilities of the crystalline samples were measured on a Quantum Design MPMS-XL. Direct-current (dc) magnetic susceptibility measurements were performed on polycrystalline samples of **1**−**7** over the temperature range 2−300 K and in an applied field of 0.1 T, respectively. The dynamics of the magnetization of complexes **1** and **3** were investigated through the alternating-current (ac) susceptibility measurements in the zero static fields and applied dc fields with a 2.0 Oe ac oscillating field.

3. Results and Discussion

3.1 Synthesis and molecular structures

Compound $H_4\mathbf{L}$ was synthesized according to the previously reported method [14], and this is outlined in Scheme 1; for the ^{1}H NMR spectrum, see Fig S1 (ESI). $H_4\mathbf{L}$ does not dissolve well in ethanol, however it dissolved readily once the nickel acetate salt was added and the solution changed from reddish brown to dark green immediately after the addition of the lanthanide metal chloride. The mixture was then filtered and kept at room temperature undisturbed for slow evaporation. Using

this method, dark green crystals of complexes **1**–**7** were obtained and were washed with cold ethanol.

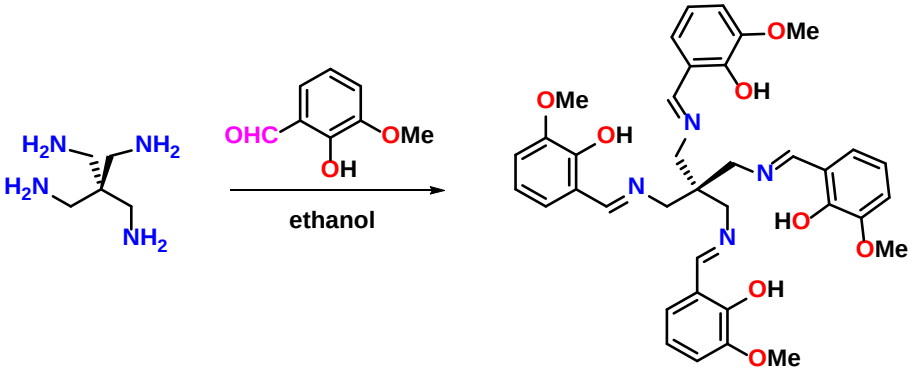

Scheme 1. Synthesis of H_4**L**.

The crystal structures of **1**–**7** were determined by single-crystal X-ray crystallography. All {Ni(II)Ln(III)}$_2$ complexes crystallized in the same triclinic space group *P*-1. The seven complexes are isomorphous with the general formula [Ni_2Ln_2(**L**)(H_2O)$_9$(OH)$_4$Cl]·3H_2O·Cl (**1**, **2**, **5**) (Ln = Dy (**1**), Tb (**2**), Ho (**5**)) or [Ni_2Ln_2(**L**)(H_2O)$_{12}$Cl]·3H_2O·5Cl (**3**, **4**, **6**, **7**) (Ln = Gd (**3**), Sm (**4**), Nd (**6**), Pr (**7**)); H_4**L** = *N*,*N*',*N*'',*N*'''-tetra(3-methoxysalicylidene)-pentaerythritol). Six chloride ions (or three chloride ions and hydroxide ions) as counterions reside in the crystal lattice, neutralizing the excess cation charge on the coordination spheres **1**–**7**. Due to their analogous structures, as a representative, only the crystal structure of **1** is discussed in detail here. The selected bond lengths and angles are listed in Tables S1 and S2 and the molecular structures of **2**–**7** are presented in the ESI (Figures S2-S7).

In complex **1** (Figure 1a), each distorted octahedral nickel centre is bound in *N*,*O*,*O*,*N*-fashion by an imine and a phenoxide of two arms of L^{4-}, which is reminiscent of the situation observed for the complex [Ni_2L]·2H_2O [14]. Additionally, in **1**, Dy(III) ions are bound to the phenoxide oxygen atoms and the oxygen of the *ortho* methoxy substituent. Within the {Ni(II)Dy(III)}$_2$, the metal-metal distances are Ni···Ni, Ni1···Dy1, Ni2···Dy2 and Dy···Dy

at 6.320 Å, 3.511 Å, 3.416 Å and 12.828 Å, respectively, whilst the Ni−O−Dy bridging angles are 105.1(2)°/104.7(2)° for the Dy1−($O_{phenoxide}$)−Ni1 motif and 105.8(3)/107.3(3)° for the Dy2−($O_{phenoxide}$)−Ni2 counterpart.

As shown in Figure 1b, two water molecules (or one water molecule and one chloride ion) coordinate to the Ni(II) ions completing the coordination sphere. The Ni−$O_{phenoxide}$ bond lengths are in the range 2.002(6)−2.043(6) Å, whereas the Ni−O_{water} bond lengths are slightly larger, with values in the range 2.134(8)−2.207(7) Å. On the other hand, the coordination sphere of Dy1 and Dy2 are completed by the *o*-vanillin derived part of ligand and water molecules. The eight-coordinate Dy1 centre exhibits what can be described as a hula hoop-like geometry, where the cyclic ring is defined by the atoms O5, O6, O7, O8 and O18 [15]. The nine-coordinate Dy2 centre exhibits an irregular muffin geometry which has O1, O2, O3, O4, O10, O11, O12, O13 and O14 placed in the nine-vertex positions [15a]. The Dy−O phenolate bond lengths (2.270(6)−2.354(7) Å) are slightly shorter than those associated with the methoxy groups (2.533(7)−2.602(8) Å). All the complexes exhibit the same coordination mode for the central metals, except for complexes **6** (S6, ESI) and **7** (S7, ESI) where both the Nd1, Nd2 and Pr1, Pr2 reveal irregular muffin geometries. Interestingly, in complex **4** (S4, ESI), two different structures are found in the asymmetric unit, one is similar to complex **1**, whereas, the another is similar to complexes **6** or **7**.

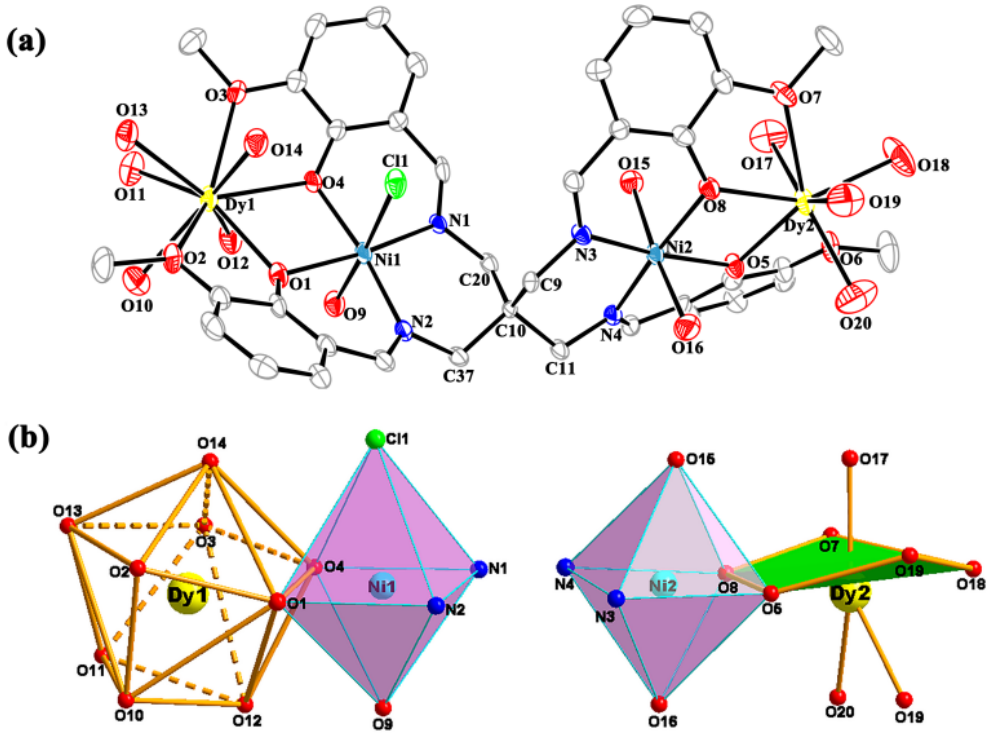

Figure 1. (a) Molecular structure of complex **1**. (b) Coordination polyhedral observed in **1**: irregular muffin geometry for Dy1, hula hoop-like geometry for Dy2 and distorted octahedral environment for Ni1 and Ni2. All hydrogen atoms and the free Cl^- anion and solvents are omitted for clarity.

The angles Ni1−Dy1−C10 and Ni2−Dy2−C10 are 178.33° and 177.77° respectively, which reveal that the central carbon atom C10 is almost in line with Ni1, Dy1 and Ni2, Dy2 respectively and the two lines are present in a V-shaped arrangement. The vertex position has the angle of Ni1−C10−Ni2 137.36°, and such an arrangement is extremely rare compared to other reported tetranuclear clusters based on $\{Ni(II)_2Dy(III)_2\}$, which tend to adopt cubane-like [16] or normal butterfly [17] type metallic cores. Moreover, the dihedral angle between the C20−C10−C37 and C9−C10−C11 planes is 89.97°. Additionally, the $Ni(O_{phenoxide})_2Dy$ metallacycles are almost planar with the dihedral angle between the O−Ni−O and O−Dy−O planes of 4.87° and 5.61° for $Ni1(O_{phenoxide})_2Dy1$ metallacycle and $Ni2(O_{phenoxide})_2Dy2$ metallacycle, respectively. The dihedral angle between the Ni1−O5−Dy1 and Ni1−O8−Dy1 planes is 6.33°. In addition, the dihedral angle between the

Ni2−O1−Dy2 and Ni2−O4−Dy2 planes is 7.49°, which reveals that the Ni2($O_{phenoxide}$)$_2$Dy2 plane is more distorted than Ni1($O_{phenoxide}$)$_2$Dy1, which likely causes the different coordination numbers at Dy. We note that different arrangements of the metallic cores can influence the magnetism of the resulting complexes.

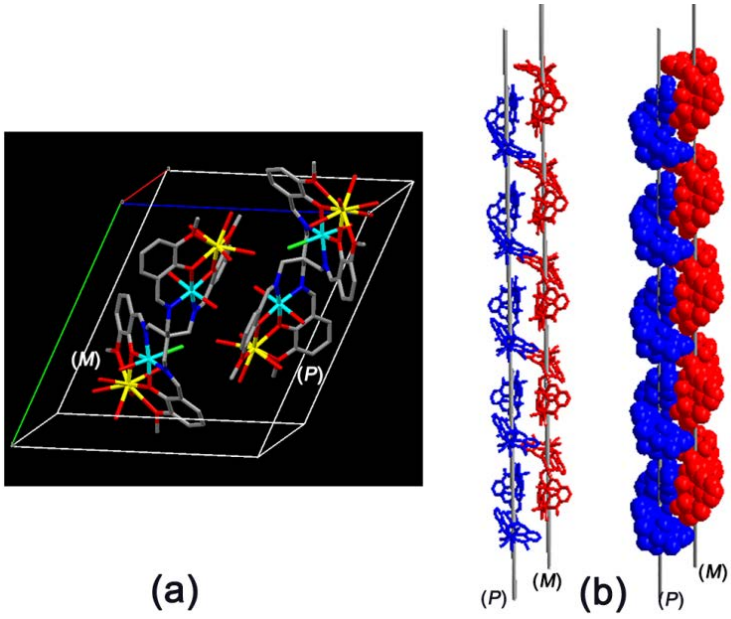

Figure 2. *M*- and *P*-helical structure of **1** in the unit cell; (b) 1D columnar structure assembled from *M*- and *P*-helical. All hydrogen atoms and the free Cl^- anion and solvents are omitted for clarity.

Interestingly, in each unit cell, a left-handed (*M*) and a right-handed (*P*) chiral conformation is present (Figure 2a). Moreover, a twisted 1D chain was formed by countless right-handed (or left-handed) helices in the same direction via intermolecular CH···π interactions and intermolecular hydrogen bond interactions. The two helical chains packed parallel, *i.e*. face-to-face, to give a racemic mixture of two enantiomeric helices as shown in Figure 2b. In recent years, the introduction of chiral properties into molecular materials is an ideal strategy for the preparation of multifunctional molecular based magnets, and magnets of this type are promising multifunctional complexes [18].

3.2 *Magnetic properties.*

The magnetic properties of the above seven complexes were investigated by utilizing the crystalline samples over the 2−300 K temperature range under an applied magnetic field of 0.1 T. The room temperature $\chi_M T$ values for complexes **1**–**7** are 29.69, 24.90, 14.98, 1.58, 27.86, 5.15, and 4.59 $cm^3\ mol^{-1}$ K, respectively, which are close to the expected values for two uncoupled Ni(II) ions and two respective Ln(III) ions (30.34, 25.64, 17.76, 2.18, 30.14, 5.28, and 5.20 $cm^3\ mol^{-1}$ K). For complex **3**, upon cooling to 30 K, the $\chi_M T$ product remains constant, and then increases to 17.58$cm^3\ mol^{-1}$ K at 7 K, following a drop to 16.43 $cm^3\ mol^{-1}$ K at 2 K, which is probably due to the competing ferromagnetic and anti-ferromagnetic interactions. For complex **5**, the $\chi_M T$ product declines slowly above 50 K, whilst the other complexes gently drop above 20 K, then all decrease distinctly to a minimum value at 2 K. This is tentatively ascribed to a combination of the depopulation of the excited Stark sublevels and non-negligible anti-ferromagnetic coupling between the adjacent metal ions [19]. The plots of *M vs. H* for complexes **1**–**7** at 2 K were obtained and are displayed in the ESI (Figure S8). For complexes **1**, **2**, **3** and **5**, the values of *M* increase rapidly from 0 to 2T, whereas for complexes **4**, **6** and **7**, relatively moderate growth was observed, and all slowed above 2T. At 8T and 2K, the value of *M* reached 21.80, 20.74, 17.31, 4.99, 21.06, 6.72 and 9.44 $N\beta$, respectively, which are smaller than the theoretical value. The approaching saturation of the magnetization indicates the possible presence of magnetic anisotropy and/or low-lying excited states. In addition, the field dependence of the magnetization *M vs. H* plots for complex **1** at different temperatures (2, 3, and 5 K) were obtained. The plot of *M vs. H/T* curves (Figure S9, inset) show non-superimposed curves, and confirm the existence of significant magnetic anisotropy and/or low-lying excited states of Dy(III) and Ni(II) ions [20].

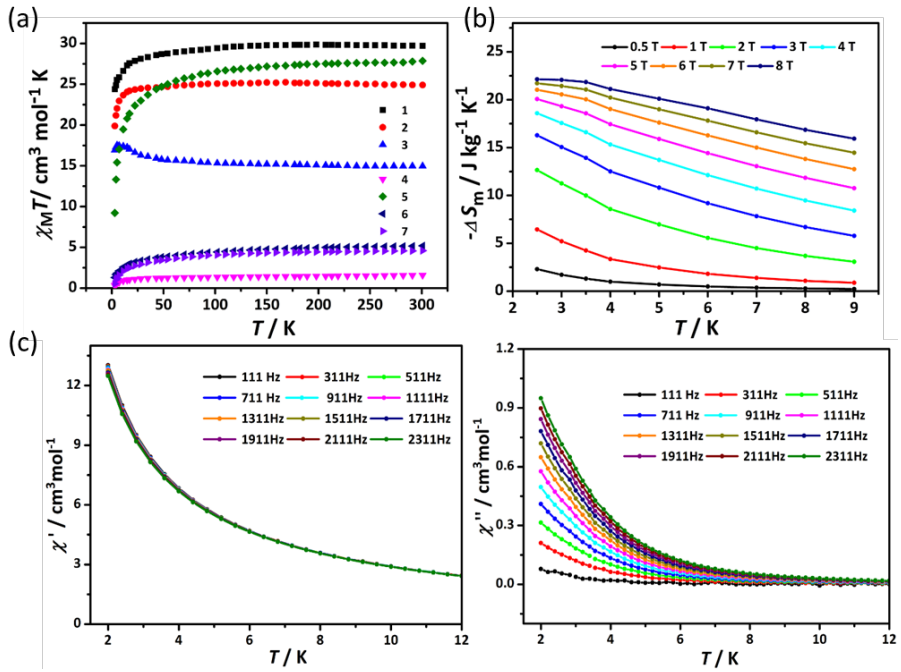

Figure 3 (a) Plots of $\chi_M T$ *vs.* T for complexes **1–7**. (b) Experimental $-\Delta S_m$ of complex **3** at various temperatures and magnetic field change. (c) Temperature dependence of the in-phase (χ') and out-of-phase (χ'') ac susceptibility data for complex **1** under a zero-dc field.

To explore the possibility of magnetic dynamics of magnetization, data for the temperature dependent alternating current (ac) susceptibility were collected under zero applied dc field. As shown in Figure 3 (and S10, ESI), the split curves in the in-phase (χ') and out-of-phase (χ'') ac susceptibility signals can only be observed in complex **1**. This illustrates the existence of the phenomenon of slow magnetic relaxation, which is a typical characteristic of single-molecule magnet [21]. However, no obvious peaks emerged due to the fast quantum tunnelling of magnetization (QTM) via the spin reversal barrier. To overcome the degeneracy of ground state and suppress the effect of QTM, an external dc field of 2000Oe was applied to survey the temperature-dependent ac susceptibilities. It was found that QTM could be partially suppressed and the maxima of χ'' could not be detected within the observable range. Similar magnetic behaviour was also presented in other reported polynuclear 3d–4f clusters with eight- or nine-coordinated lanthanide ions [22], but rarely

observed for linear systems. Therefore, the relaxation time (τ0) and effective energy barrier (U_{eff}) cannot be simulated by the traditional Arrhenius method. However, rough values of τ0 and U_{eff} could be obtained by use of the model of Debye using the equation $\ln(\chi''/\chi') = \ln(\omega\tau 0) + E_a/kBT$ [23]. This supposes only one relaxation process in complex **1**, an estimated U_{eff} of 1.30 K and τ0 of 4.12×10^{-6}s were provided for the optimal linear fit (Figure S11, ESI). The τ0 value is consistent with the typical range for SMMs (10^{-6}–10^{-11} s) [24]. The relatively small energy barrier might be assigned to the low symmetry of the coordination configuration of Dy(III) ions in the final structure.

The magnetocaloric behaviour of complex **3** was investigated because the apparent ferromagnetic interactions between the Gd(III) and Ni(II) ions and the isotropic Gd(III) ions and only second-order anisotropic Ni(II) might create a relatively significant magnetocaloric effect. The magnetic entropy change ΔS_m parameter was explored for complex **3** based on the magnetization data (Figure S12, ESI) by applying the Maxwell equation of $\Delta Sm(T)_{\Delta H} = \int [\partial M(T,H)/\partial T]_H \, dH$ (Figure 3) [25]. As shown in Figure 3b, the calculated maximum value of $-\Delta S_m$ was calculated as 22.14 J kg^{-1} K^{-1} at 2.5 K and 8 T. As expected, the experimental value (22.14 J kg^{-1} K^{-1}) is smaller the theoretical one (31.08 J kg^{-1} K^{-1}) calculated by the equation $-\Delta S_m = nR \ln(2S + 1)$. This may be ascribed to the weak anti-ferromagnetic interaction between adjacent metal ions, crystal-field effects as well as the anisotropy of the Ni(II) ion. Moreover, the extracted $-\Delta S_m$ value is larger than that observed for other reported Ni_2Gd_2 complexes of similar molecular mass, and even comparable to those of reported high nuclearity heterometallic clusters, suggesting that complex **3** is a potential molecular magnetic cooling material.

4. Conclusions

In summary, a series of tetranuclear 3d–4f heterometallic [Ln_2Ni_2] clusters based on a multidentate tetra-branched Schiff base ligand set have been prepared and structurally

characterized. Two [LnNi] units bearing different coordination environments are distributed on either side, connected by a central carbon (C10) atom, forming a twisted "butterfly" configuration. Magnetic results reveal the existence of ferromagnetic coupling in complex **3** and dominant anti-ferromagnetic interactions in the other six complexes. The Dy derivative should be regarded as a type of SMM due to the presence of slow magnetic relaxation under zero applied dc field with a small effective energy barrier of 1.30 K. Moreover, the Gd derivative exhibit a significant magnetocaloric effect with 22.14 J kg^{-1} K^{-1} at 2.5 K and 8T.

Acknowledgements

This work was supported by the National Natural Science Foundation of China (22065009, 22066007), Guizhou Provincial Natural Science Foundation (grant number [2019] 2792], grant number ZK[2021]076 and grant number 19NSP035) and Hubei Provincial Natural Science Foundation of China (2020CFB475). CR thanks the EPSRC for an Overseas Travel Grant (EP/R023816/1).

Appendix A. Supplementary data

Electronic Supplementary Information (ESI) available. Detailed experimental description, characterization and physical measurements (PDF). X-ray crystallographic data for the seven complexes (CIF). CCDC 2114035–2114041 contain the supplementary crystallographic data for **1-7**. These data can be obtained free of charge via http://www.ccdc.cam.ac.uk/conts/retrieving.html.

References

[1] (a) R. E. P. Winpenny, Chem. *Soc. Rev*. 27 (1998) 447.

(b) C. Benelli and D. Gatteschi, *Chem. Rev*., 102 (2002) 2369.

(c) R. Sessoli and A. K. Powell, *Coord. Chem. Rev.* 253 (2009) 2328.

(d) L. Sorace, C. Benelli and D. Gatteschi, *Chem. Soc. Rev*. 40 (2011) 3092.

[2] (a) M. Evangelisti and E. K. Brechin, *Dalton Trans*. 39 (2010) 4672.

(b) E. Cremades, S. Gomez-Coca, D. Aravena, S. Alvarez and E. Ruiz, *J. Am. Chem. Soc*. 134 (2012) 10532.

(c) J. W. Sharples and D. Collison, *Polyhedron* 2013, 54 (2013) 91.

(d) Y.-Z. Zheng, G.-J. Zhou, Z. Zheng and R. E. P. Winpenny, *Chem. Soc. Rev.* 43 (2014) 1462.

[3] (a) P. H. Guo, J. L. Liu, J. H. Jia, J. Wang, F. S. Guo, Y.C. Chen, W. Q. Lin, J. D. Leng, D. H. Bao, X. D. Zhang, J. H. Luo and M. L. Tong, *Chem. - Eur. J*. 19 (2013) 8769.

(b) I. J. Hewitt, J. K. Tang, N. T. Madhu, C. E. Anson, Y. H. Lan, J. Luzon, M. Etienne, R. Sessoli and A. K. Powell, *Angew. Chem., Int. Ed*. 49 (2010) 6352.

(d) J. L. Liu, Y. C. Chen and M. L. Tong, *Chem. Soc. Rev.* 47 (2018) 2431.

(e) Y. S. Meng, S. D. Jiang, B. W. Wang and S. Gao, *Acc. Chem. Res*. 49 (2016) 2381.

[4] (a) M. N. Leuenberger and D. Loss, *Nature,* 410 (2001) 789.

(b) M. Affronte, *J. Mater. Chem*. 19 (2009) 1731.

(c) A. Candini, S. Klyatskaya, M. Ruben, W. Wernsdorfer and M. Affronte, *Nano Lett.* 11 (2011) 2634.

(e) R. Vincent, S. Klyatskaya, M. Ruben, W. Wernsdorfer and F. Balestro, *Nature*, 488 (2012) 357.

[5] (a) C. Benelli and D. Gatteschi, *Chem. Rev.* 102 (2002) 2369.

(b) E. Moreno Pineda, N. F. Chilton, F. Tuna, R. E. P. Winpenny and E. J. L. McInnes, *Inorg. Chem*. 54 (2015), 5930.

[6] (a) T. D. Pasatoiu, J.-P. Sutter, A. M. Madalan, F. Z. C. Fellah, C. Duhayon and M. Andruh, *Inorg. Chem.* 50 (2011) 5890.

(b) S. Pei, Z. Hu, Z. Chen, S. Yu, B. Li, Y. Liang, D. Liu, D. Yao and F. Liang, *Dalton Trans.* 47 (2018) 1801.

[7] L. Zhao, J. Wu, H. Ke and J. Tang, *Inorg. Chem.* 53 (2014) 3519.

[8] (a) L. Jiang, Y. Liu, X. Liu, J. Tian and S. Yan, *Dalton Trans*. 46 (2017) 12558.

(b) H. Ke, L. Zhao, Y. Guo and J. Tang, *Inorg. Chem.* 51 (2012) 2699.

[9] (a) M. Biswas, E. C. Sañudo and D. Ray, *Inorg. Chem.* 60 (2021) 11129.

(b) P. Hu, X.-n. Wang, C.-g. Jiang, F. Yu, B. Li, G.-l. Zhuang and T. Zhang, *Inorg. Chem.* 57 (2018) 8639.

(c) K.-Q. Hu, X. Jiang, S.-Q. Wu, C.-M. Liu, A.-L. Cui and H.-Z. Kou, *Inorg. Chem.* 54 (2015) 1206-1208.

[10] G. M. Sheldrick, Program SADABS: Area-Detector Absorption Correction, University of Göttingen, Germany. 1996.

[11] G. M. Sheldrick, *Acta Crystallogr., Sect. C: Cryst. Struct. Commun*. 71 (2015) 3.

[12] O. V. Dolomanov, L. J. Bourhis, R. J. Gildea, J. A. K. Howard and H. *J.* Puschmann, *Appl. Cryst.* 42 (2009) 339.

[13] A. L. Spek, *Acta Cryst.* C71 (2015) 9.

[14] G.-Q. Jiang, R. Wang, L.-L. Long, T. Sun, Z.-c. Yang, Y.-Q. Zhang and Q.-J. Zhang, *J. Coord. Chem*. 69 (2016) 678.

[15] (a) A. Ruiz-Martínez, D. Casanova and S. Alvarez, *Chem. – Eur. J.* 14 (2008) 1291.

(b) Y.-N. Guo, G.-F. Xu, W. Wernsdorfer, L. Ungur, Y. Guo, J. Tang, H.-J. Zhang, L. F. Chibotaru and A. K. Powell, *J. Am. Chem. Soc*. 133 (2011) 11948.

[16] (a) Y. Gao, L. Zhao, X. Xu, G. Xu, Y. Guo, J. Tang and Z. Liu, *Inorg. Chem.* 50 (2011) 1304.

(b) Z. Meng, F. Guo, J. L. Liu, J. Leng and M. Tong, *Dalton. Trans*. 41 (2012) 2320.

(c) W. R. Yu, G. H. Lee and E. C. Yang, *Dalton. Trans*. 42 (2013) 3941.

[17] (a) K. C. Mondal, G. E. Kostakis, Y. Lan, W. Wernsdorfer, C. E. Anson and A. K. Powell, *Inorg. Chem*. 50 (2011) 11604.

(b) X. Li, F. Min, C. Wang, S. Lin, Z. Liu and J. Tang, *Inorg. Chem.* 54 (2015) 4337.

(c) Y. Song, J. Li, R. Wei, T. Pu, F. Cao, L. Yang, Y. Han, Y. Zhang and J. Zuo, *Inorg. Chem. Front*. 4 (2017) 114.

[18] (a) T. Kimura, T. Goto, H. Shintani, K. Ishizaka, T. Arima and Y. Tokura, *Nature,* 426 (2003) 55.

(b) H. Kumagai and K. Inoue, *Angew. Chem., Int. Ed*. 38(1999) 1601.

(c) M. Minguet, D. Luneau, E. Lhotel, V. Villar, C. Paulsen, D. B. Amabilino and J. Veciana, *Angew. Chem., Int. Ed*. 41 (2002) 586.

(e) K. Inoue, H. Imai, P. S. Ghalasaki, K. Kikuchi, M. Ohba, H. Ohkawa, and J. V. Yakhmi, *Angew. Chem., Int. Ed.* 40 (2001) 4242.

(f) H. Imai, K. Inoue, K. Kikuchi, Y. Yoshida, M. Ito, T. Sunahara and S. Onaka, *Angew. Chem., Int. Ed*. 43 (2004) 5618.

[19] (a) Y. Liu, Z. Chen, J. Ren, X. Q. Zhao, P. Cheng and B. Zhao, *Inorg. Chem*. 51 (2012) 7433.

(b) Y. Zheng, X. J. Kong, L. S. Long, R. B. Huang and L. S. Zheng, *Dalton Trans*. 2011, 40 (2011) 4035.

(c) L. B. Escobar, G. P. Guedes, S. Soriano, R. A. Cassaro, J. Marbey, S. Hill, M. A. Novak, M. Andruh and M. G. Vaz, *Inorg. Chem*. 57 (2018) 326.

[20] (a) S. Mukherjee, J. Lu, G. Velmurugan, S. Singh, G. Rajaraman, J. Tang and S. K. Ghosh, *Inorg. Chem*. 55 (2016) 11283.

(b) H. Ke, X. Lu, W. Wei, W. Wang, G. Xie and S. Chen, *Dalton Trans*. 46 (2017) 8138.

[21] J. L. Liu, W. Q. Lin, Y. C. Chen, J. D. Leng and F. S. Guo, *Inorg. Chem*. 52 (2013) 457.

[23] (a) D. I. Alexandropoulos and S. Mukherjee, *Inorg. Chem*. 50 (2011) 11276.

(b) C. J. Kuo, R. J. Holmberg and P. H. Lin, *Dalton Trans*. 44 (2015) 19758.

(c) T. Lacelle, G. Brunet, R. J. Holmberg, B. Gabidullin and M. Murugesu, *Cryst. Growth Des.* 17 (2017) 5044.

(d) H. S. Wang, F. J. Yang, Q. Q. Long, Z. Y. Huang, W. Chen, Z. Q. Pan and Y. Song, *Dalton Trans*. 45 (2016) 18221.

(e) X. Q. Zhao, J. Wang, D. X. Bao, S. Xiang, Y. J. Liu, Y. C. Li, *Dalton Trans*. 46 (2017) 2196.

[23] S. Y. Lin, L. Zhao, Y. N. Guo, P. Zhang, Y. Guo and J. Tang, *Inorg. Chem*. *51* (2012) 10522.

[24] (a) S. K. Langley, N. F. Chilton, L. Ungur, B. Moubaraki, L. F. Chibotaru and K. S. Murray, *Inorg. Chem*. 51 (2012) 11873.

(b) C. M. Liu, D. Q. Zhang and D. B. Zhu, *Inorg. Chem*. 52 (2013) 8933.

(c) X. F. Ma, Z. Wang, X. L. Chen, M. Kurmoo and M. H. Zeng, *Inorg. Chem.* 56 (2017) 15178.

[25] (a) M. Evangelisti, F. Luis, L. J. de Jongh and M. Affronte, *J. Mater. Chem*. 16 (2006) 2534.

(b) R. Sessoli, *Angew. Chem., Int. Ed.* 51(2012) 43.

(c) M. Zhang, T. Yang, Z. Wang, X. F. Ma, Y. Zhang, S. M. Greer, S. A. Stoian, Z. W. Ouyang, H. Nojiri, M. Kurmoo and M. H. Zeng, *Chem. Sci*. 8 (2017) 5356.